FERMILAB-PUB-19-053
ACCEPTED

Assembly of a Mechanical Model of MQXFB, the 7.2 m Long Low-β Quadrupole for the High Luminosity LHC Upgrade

G. Vallone, G. Ambrosio, E. Anderssen, N. Bourcey, D. W. Cheng, P. Ferracin, P. Grosclaude, M. Guinchard, S. Izquierdo Bermudez, M. Juchno, F. Lackner, H. Pan, J.C. Perez, S. Prestemon, M. Semeraro, S. Triquet

***Abstract*—The Nb_3Sn low-β quadrupole MQXF is being developed as a part of the High-Luminosity LHC upgrade project. The magnet will be produced in two different configurations, sharing the same cross-section but with different lengths. A $7.2\,\mathrm{m}$ mechanical model of MQXFB was recently assembled at CERN with one copper coil, two low-grade coils and one rejected coil. Coil dimensions were measured with a portable Coordinate Measurement Machine. The coil pack shimming was designed in order to optimize the field quality and the contacts between the coils and the collars. The azimuthal preload target was defined using the short models experience. The mechanical behavior during loading was monitored by means of strain gauges. The results demonstrated that the structure can provide the required prestress to the coils.**

***Index Terms*—High Luminosity LHC, Low-β quadrupole, Nb_3Sn magnet, Mechanical Model.**

I. Introduction

As part of the High-Luminosity upgrade [1] the LHC inner triplet quadrupoles will be substituted with new Nb_3Sn magnets. The Q1 and Q3 quadrupoles will be each made of two MQXFA magnets, with a magnetic length of $4.2\,\mathrm{m}$. The Q2 quadrupoles will be instead made of two MQXFB magnets, having a magnetic length of $7.15\,\mathrm{m}$ [2], [3]. MQXFA and MQXFB will share the same cross-section, shown in Fig. 1, and will produce an ultimate gradient of $143.2\,\mathrm{T/m}$ in a $150\,\mathrm{mm}$ aperture, when powered at $17.89\,\mathrm{kA}$. The design was tested in four short models [4]: the MQXFS1 [5], [6], MQXFS5 [7] and MQXFS4 [8] magnets successfully reached the ultimate current, while MQXFS3 [7] did not.

The design employs the bladder and key technology to apply the azimuthal prestress to the coils [9]. The longitudinal prestress is realized with rods, stretched by a piston and locked in place with nuts and bolts. Different loading conditions were tested during the short model campaign, exploring the impact on the magnet performances [10]–[12]. These results can be used as a reference, since scaling from $1.5\,\mathrm{m}$ to $4.2\,\mathrm{m}$ and $7.15\,\mathrm{m}$ should not affect the azimuthal mechanical performances [13]. On the other hand, a longer magnet will reduce the longitudinal stiffness of the coil. However, the numerical results presented in [14] suggest that, even if the total coil elongation scales with the magnet length, the contact pressure between the coil and the pole/spacers in the end regions should not be subject to major changes.

This paper summarizes the assembly results of a MQXFB mechanical model, built at CERN using coils without full performance, in order to verify the assembly procedures, test the mechanical soundness of the first MQXFB structure, and verify if an acceptable preload condition could be reached. The mechanical model discussed is the longest magnet assembly ever performed with the bladder and key technology.

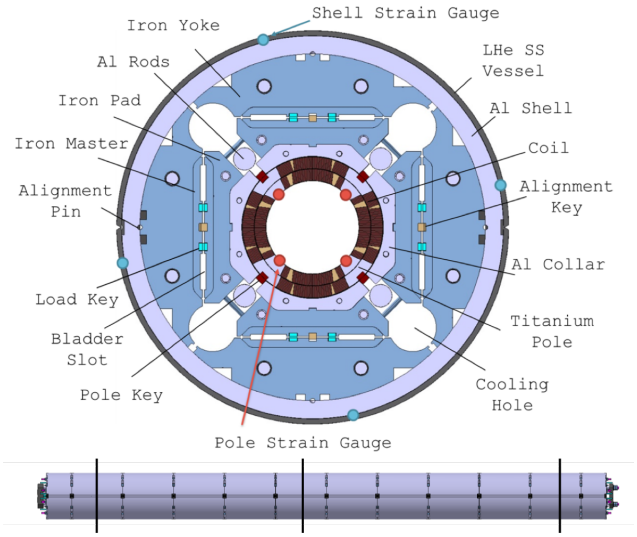

Fig. 1. MQXF cross-section (top), and MQXFB longitudinal view (bottom). The strain gauges were installed on the shell and the winding poles, as shown by the circular markers. The vertical lines in the bottom view provide their longitudinal position.

II. Coil Dimensional Measurements

MQXFB coils are being manufactured at CERN [15]: up to now eight coils were manufactured, of which four will be used for the first MQXFB prototype. A measurement machine

Automatically generated dates of receipt and acceptance will be placed here
This work was supported by the High Luminosity LHC Project at CERN and by the DOE through the U.S. LHC Accelerator Research Program.
G. Vallone, E. Anderssen, D. W. Cheng, M. Juchno, H. Pan and S. Prestemon are with Lawrence Berkeley National Laboratory, Berkeley, CA 94720 USA (e-mail: gvallone@lbl.gov).
G. Ambrosio is with the Fermi National Accelerator Laboratory, Batavia, IL 80510 USA.
N. Bourcey, P. Ferracin, P. Grosclaude, M. Guinchard, S. Izquierdo Bermudez, J.C. Perez, M. Semeraro and S. Triquet are with the European Organization for Nuclear Research (CERN), 1211 Geneva, Switzerland.
Colour versions of one or more of the figures in this paper are available online at http://ieeexplore.ieee.org.
Digital Object Identifier: xx

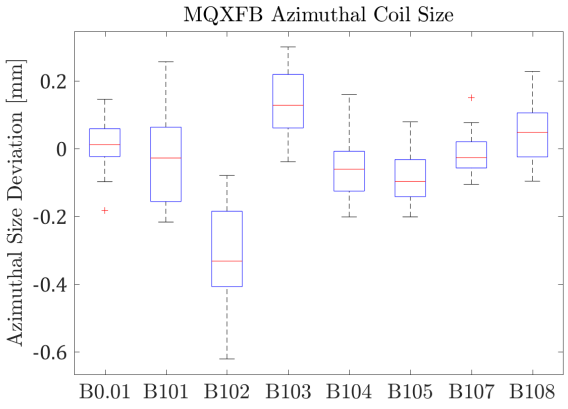

Fig. 2. Box plot for the azimuthal excess of all the MQXFB coils produced up to now.

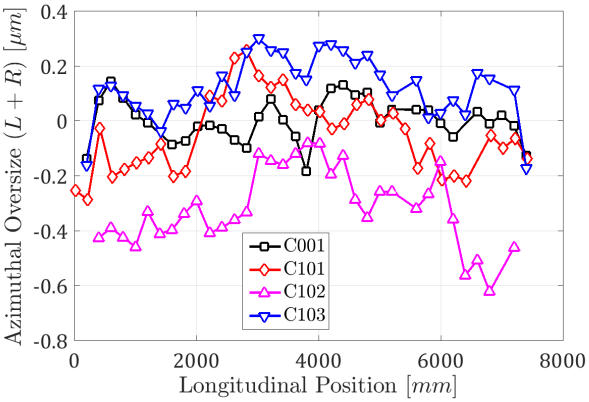

Fig. 3. Azimuthal size deviation along the coil length. The average variation is 0 µm, −300 µm, −50 µm and 150 µm for Coil C001, C101, C102 and C103 respectively. The size deviation from the average is contained within ±250 µm.

was used to probe the outer radius, the pole and the mid-planes of the coil. The operation was repeated every 200 mm, scanning 37 cross-sections in total. Similarly to what was done for the short models [16], the cross-sections were aligned against a CAD model, computing the local azimuthal excess $(L + R)$. A box plot of its deviation is shown in Fig. 2 for all the MQXFB coils produced up to now. For the mechanical assembly the following coils were selected: C001, a copper coil; C101 and C102, two low-grade coils; C103, a rejected coil, damaged during the reaction process [15]. Their size variation along the length is shown in Fig. 3. The average variation is 0 µm, −300 µm, −50 µm and 150 µm for Coil C001, C101, C102 and C103 respectively. The variation along the length of each coil is contained within about ±250 µm. This is more than two times the variation measured on the short models [16]. Following the procedure proposed in [12] the estimated azimuthal stress variation in the coils (measured at the pole inner layer) would be in the order of ±40 MPa, twice the one measured on the short models.

In order to improve the coil geometry stringent care was put on the procedure, in particular the pressure and torque applied on the curing, reaction, impregnation fixtures. The

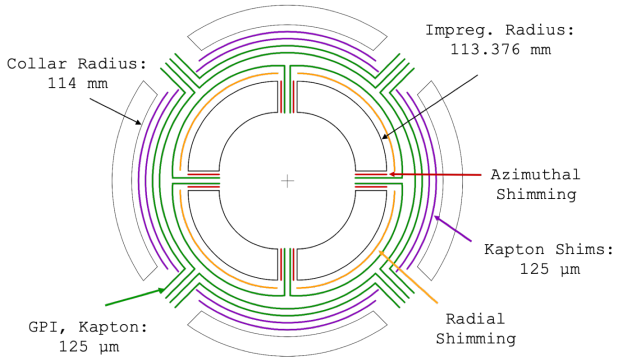

Fig. 4. Standard shimming applicable for the MQXF magnets. One 125 µm ground insulation polyamide layers is wrapped around the coil, and two around the collars. Two additional layers are foreseen to match the nominal coil radius to the collar one. The plot also shows the azimuthal and radial shimming options.

TABLE I
FIELD QUALITY VARIATION AS A FUNCTION OF THE COIL ORDERING

Ordering†	1	2	3	4	5	6
b_3	-1.1	0.9	-1.1	-0.2	0.9	-0.2
b_5	2.2	-1.8	2.2	0.4	-1.8	0.4
a_3	0.2	0.2	-0.9	-0.9	1.1	1.1
a_4	-2.9	3.6	0.7	3.6	0.7	-2.9
a_5	0.4	0.4	-1.8	-1.8	2.2	2.2

† 1: C001 C101 C102 C103 ‖ 2: C001 C101 C103 C102 ‖ 3: C001 C102 C101 C103 ‖ 4: C001 C102 C103 C011 ‖ 5: C001 C103 C101 C102 ‖ 6: C001 C103 C102 C101.

impregnation process itself was also improved refining the process parameters. The coil dimensional uniformity improved, as visible from Fig. 2: the variation for the latest coils is contained within ±150 µm.

III. COIL PACK ASSEMBLY

The nominal outer radius of the MQXF coils is equal to 113.376 mm, 0.625 mm smaller than the collars inner radius.

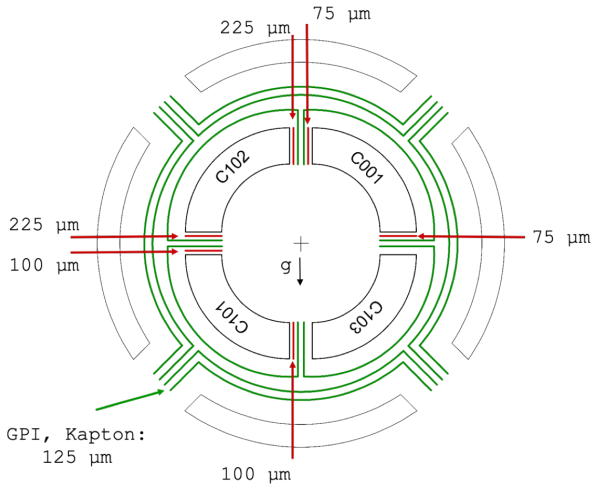

Fig. 5. Shimming plan and coil positioning adopted for the mechanical assembly. A 150 µm distance was left between the nominal collar radius and the coil and shim package.

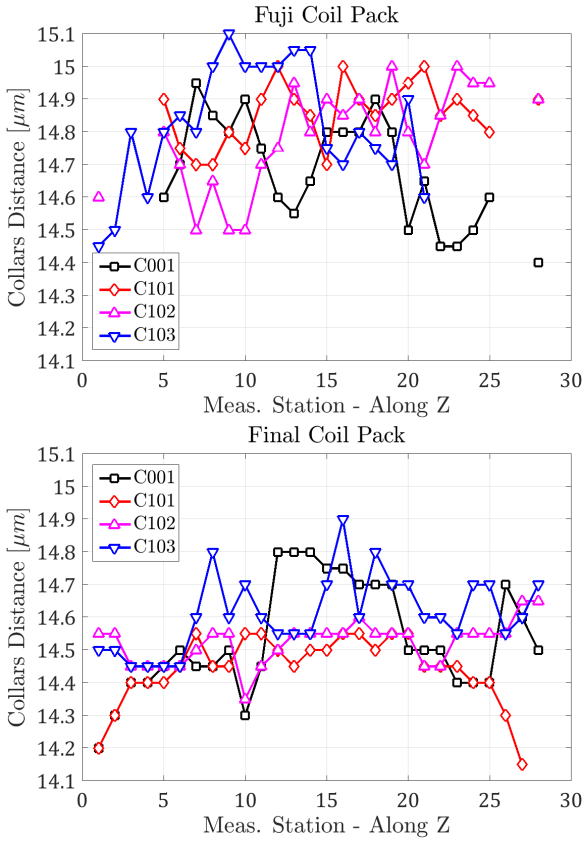

Fig. 6. Gaps between the collars as measured after the pressure sensitive film assembly (top), and after the final assembly (bottom). The insertion of the pole keys improved the overall alignment, decreasing the gaps variation.

This gap can be filled with radial polyamide shims, in the configuration shown in Fig. 4. In particular, three polyamide shims with a total thickness of 375 µm constitute the ground plane insulation, and two optional sheets can fill the remaining space, allowing to accommodate oversized coils. Positioning errors due to smaller coils can also be corrected, by means of radial and azimuthal (mid-plane) shims. The azimuthal solution is in general preferred, as it allows to bring the four coils inner surface at the same radius, with beneficial effects on the field homogeneity [17]. As a consequence, no shimming was applied on coil C103, and mid-plane shims were applied on the other coils to match its azimuthal size.

Even if not relevant for this mechanical assembly, the relative coil positions were defined trying to obtain best possible field quality. A numerical analysis was performed, introducing the deformed coil geometry in a ROXIE [18] model, assuming a full mid-plane shimming strategy and then combining the coils with different ordering. The main effects of the coil ordering on the harmonics are resumed in Table I. The configurations labelled as 3 and 5 are equivalent, while the other configurations show a large a_4, equal to 3.6 units for sets 2, 4; -2.9 units for the configurations 1 and 5. Configuration 3 was selected. The final shimming resulting from these choices is shown in Fig. 5.

The coil pack formed in this way is about 100 µm bigger than the nominal one in the radial direction. To accommodate

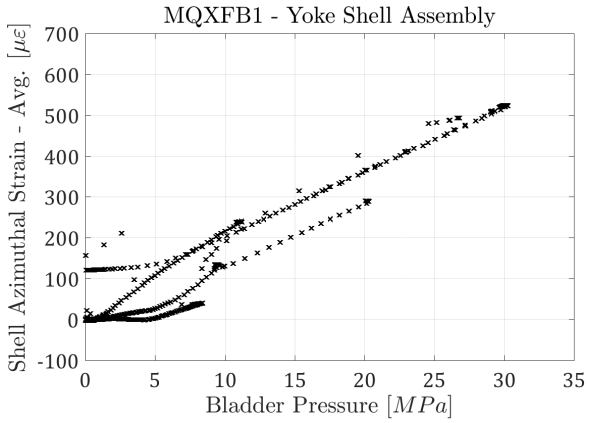

Fig. 7. Yoke-shell module sub-assembly: measured shell strain for one of the central modules as a function of the bladder pressure applied.

for this is possible to remove part of the radial shims. The contact quality was verified in a first coil pack where a layer of pressure sensitive film (Fuji paper) was inserted between the coils and the collars. Both the strain gauge data and the pressure sensitive film analysis suggested an imperfect contact of coils and collars. It was shown in the past that this could produce bending at the inner layer pole [13]. As a consequence, a further space of 150 µm was then left, in an attempt of optimizing the coil-collar contact. This value is similar to the one left in most MQXF magnets [19], [20].

The distance between the collar sides was measured at several locations along the length of the magnet, as shown in Fig. 6. For the Fuji assembly the alignment pole key was not inserted. The variation along the length of these gaps was very close to the one measured on the short models, and contained within ±300 µm in the magnet straight section. This measurement allows to compute the expected gap on the alignment pole key sides, and to add shims if required. This distance is in fact defines the relationship between the amount of force produced by the structure and the one absorbed by the coils [11]. Using the measurements from the first assembly the expected gap would have been equal to 400 µm. However, as the radial shimming was reduced in the second and final assembly (Fig. 5), so was the azimuthal space between the collars. An additional assembly without alignment pole key would have been necessary to correctly measure the collar distances, but was not performed. As a consequence, the measurements can not be directly compared with the short model ones. The gap measured between the pole key sides was equal to 100 µm in total. No shim was applied to the pole key. The variation along the straight section was found equal to ±200 µm: the variation decrease was probably due to the presence of the pole keys, showing the expected effect in improving the coil-pack alignment.

IV. Support Structure Assembly and Preload

The MQXFB yoke and shells subassembly is in five modules: two lateral modules made of three shells, and three central modules with two shells each (see Fig. 1). Each module was assembled stretching the shell by means of bladders

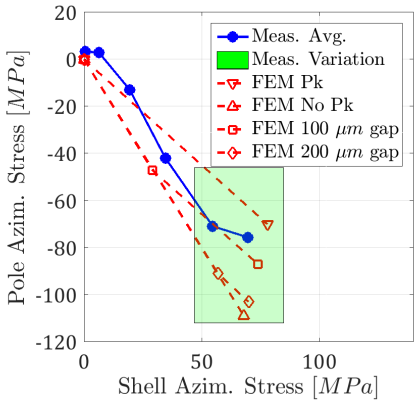

Fig. 8. Shell and azimuthal stress during the preloading operation. The plot shows the average values across all the measuring locations, their variation, and three FE reference models with different contact conditions between the alignement pole key and the collar sides.

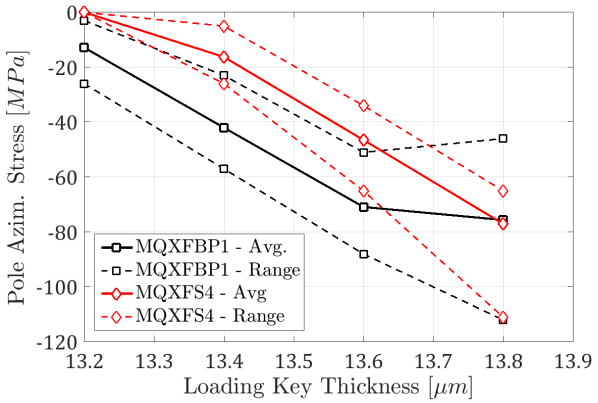

Fig. 9. Pole azimuthal stress increase as a function of the pole key thickness for the last short model tested, MQXFS4, and for the MQXFB mechanical assembly.

inserted in the cooling holes, and then locking the yokes in place with the yoke keys. The shell strain as a function of the bladder pressure for one of the central modules is shown in Fig. 7. The operation required a pressure of about 30 MPa, with a maximum strain in the shells of 600 µm/m, and a final strain in the order of 100 µm/m. The modules were then connected by means of longitudinal rods inserted in the yoke.

The coil pack was then inserted in the yoke-shell subassembly, the masters packages were slit inside, and the azimuthal loading system was installed. The loading operation was performed inserting keys of increasing thickness inside the structure. In [14], the target prestress for the MQXFB magnets was defined to be, after cooldown, equal to 150 MPa. This prestress is in fact the one that would avoid any pole unloading up to the ultimate current. The successful performances of short models with lower prestress suggest that this prestress could in fact be non-necessary. As a consequence, the target prestress was defined to be as close as possible to the one of the latest model tested, MQXFS4: 76 MPa at warm, 106 MPa at cold [12].

The loading results are resumed in Fig. 8 using the so-called Transfer Function (TF), defined in [10]. Along with the measured values and their variation across the available strain gauges, the graph provides the simulated TF for different contact conditions between the collars and the alignment pole keys. The measured average lies in between the upper and lower simulation limits, assuming respectively a key always and never in contact with the collar sides. This is consistent with the measured gap (see Section III). The final average prestress reached is 76 MPa, by coincidence identical to the one applied in MQXFS4. The variation across the four coils and the three measuring location is equal to ±33 MPa, larger to the one measured on the short models. The variation is roughly in line with the predictions from the coil metrological measurements. This would allow in future, for the MQXFB production, to formulate an acceptance criteria for coils. Also the shell stress variation is larger than the short models one, and equal to ±20 MPa.

The variation of pole stress as a function of the loading key thickness is shown in Fig. 9, along with the same measurements for the MQXFS4 magnet. The final thickness of the loading keys inserted was 13.8 mm for both magnets. The repeatability of this transfer function could allow to control the loading process on the basis of the sole pole key thickness. This could be fundamental for the series assemblies, where the pole strain gauges might not be installed [12]. The MQXFB model loading required a maximum bladder pressure of 37 MPa.

V. Conclusion

The MQXFB mechanical assembly confirmed the feasibility of assembling the MQXFB magnet following the procedure already developed on the MQXF short models. The test allowed also to test the performances of the first MQXFB support structure.

One copper coil, two low grade coils and a faulty coil were used in the assembly. The measured coil azimuthal size deviation from the average was within ±250 µm. Computations suggest that this could produce a stress variation of ±40 MPa. Improvements of the coil fabrication process allowed to bring this deviation within ±150 µm.

Field quality considerations allowed to define the coil relative positioning and the amount and typology of the shims. No significant difference was noticed with the short models on the structural alignment as measured on the collar sides. When the coil pack was assembled with the keys the collar sides distance variation decreased, suggesting an improvement in the longitudinal alignment.

The final measured average prestress was 76 MPa, identical to the MQXFS4 value, as desired. The loading key thickness was also the same, 13.8 mm. The variation of the coil stress was contained within ±33 MPa. As expected, this value is significantly larger than what was measured on the short models.

References

[1] L. Rossi and O. Brüning, "High Luminosity Large Hadron Collider: a description for the European Strategy Preparatory Group," CERN, Geneva, Swtizerland, CERN-ATS-2012-236, 2012.

[2] E. Todesco *et al.*, "Design studies for the low-β quadrupoles for the LHC luminosity upgrade," *IEEE Transactions on applied superconductivity*, vol. 23, no. 3, 2013, Art. ID 4002405.

[3] P. Ferracin *et al.*, "Development of MQXF: The Nb_3Sn low-β quadrupole for the HiLumi LHC," *IEEE Transactions on Applied Superconductivity*, vol. 26, no. 4, pp. 1–7, 2016.

[4] P. Ferracin *et al.*, "The HL-LHC low-β quadrupole magnet MQXF: from short models to long prototypes," *IEEE Transactions on Applied Superconductivity*, 2018, Under Review.

[5] G. Chlachidze *et al.*, "Performance of the first short model 150-mm-aperture Nb_3Sn quadrupole MQXFS for the High-Luminosity LHC upgrade," *IEEE Transactions on Applied Superconductivity*, vol. 27, no. 4, pp. 1–5, Jun. 2017.

[6] S. Stoynev *et al.*, "Summary of test results of MQXFS1 - the first short model 150 mm aperture Nb_3Sn quadrupole for the High-Luminosity LHC upgrade," *IEEE Transactions on Applied Superconductivity*, vol. 28, no. 3, pp. 1–5, 2018.

[7] H. Bajas *et al.*, "Test result of the short models MQXFS3 and MQXFS5 for the HL-LHC upgrade," *IEEE Transactions on Applied Superconductivity*, vol. 28, no. 3, pp. 1–6, 2018.

[8] F. J. Mangiarotti *et al.*, "To be defined," *IEEE Transactions on Applied Superconductivity*, 2018, Under Review.

[9] S. Caspi *et al.*, "The use of pressurized bladders for stress control of superconducting magnets," *IEEE Transactions on Applied Superconductivity*, vol. 11, no. 1 II, pp. 2272–2275, 2001.

[10] G. Vallone *et al.*, "Mechanical performance of short models for MQXF, the Nb_3Sn low-β quadrupole for the Hi-Lumi LHC," *IEEE Transactions on Applied Superconductivity*, pp. 1–5, 2016.

[11] G. Vallone *et al.*, "Mechanical analysis of the short model magnets for the Nb_3Sn low-β quadrupole mqxf," *IEEE Transactions on Applied Superconductivity*, vol. 28, no. 3, pp. 1–6, 2018.

[12] G. Vallone *et al.*, "Summary of the mechanical performances of the 1.5 long models of the nb3sn low-fffdfffd quadrupole mqxf," *IEEE Transactions on Applied Superconductivity*, 2018, Under Review.

[13] P. Ferracin *et al.*, "Mechanical performance of the LARP Nb_3Sn quadrupole magnet LQS01," *IEEE Transactions on Applied Superconductivity*, vol. 21, no. 3, pp. 1683–1687, Jun. 2011.

[14] G. Vallone *et al.*, "Mechanical design analysis of MQXFB, the 7.2 m long low-β quadrupole for the High-Luminosity LHC upgrade," *IEEE Transactions on Applied Superconductivity*, vol. 28, no. 3, pp. 1–5, 2018.

[15] F. Lackner *et al.*, "Status of the long MQXFB Nb_3Sn coil prototype production for the HiLumi LHC," *IEEE Trans. Appl. Supercond*, vol. 27, no. 4, 2017.

[16] J. F. Troitino *et al.*, "Applied metrology in the production of superconducting model magnets for particle accelerators," *IEEE Transactions on Applied Superconductivity*, vol. 28, no. 3, pp. 1–6, 2018.

[17] S. I. Bermudez *et al.*, "Geometric field errors of short models for MQXF, the Nb_3Sn low-β quadrupole for the high luminosity LHC," *IEEE Transactions on Applied Superconductivity*, 2017, Under Review.

[18] S. Russenschuck, "ROXIE: Routine for the optimization of magnet X-sections, inverse field calculation and coil end design.," *Proc. 6th Eur. Particle Accelerator Conf.*, 1999.

[19] H. Pan *et al.*, "Assembly tests of the first Nb_3Sn low-β quadrupole short model for the Hi-Lumi LHC," *IEEE Transactions on Applied Superconductivity*, vol. 26, no. 4, pp. 1–5, Jun. 2016.

[20] D. W. Cheng *et al.*, "Fabrication and assembly performance of the first 4.2 m MQXFA magnet and mechanical model for the Hi-Lumi LHC upgrade," *IEEE Transactions on Applied Superconductivity*, vol. 28, no. FERMILAB-PUB-17-372-TD, 2018.